Bubble Collapse Propagation and Pressure Wave at Periodic Cloud Cavitation

Yasuhiro Saito and Keiichi Sato

Kanazawa Institute of Technology, Department of Mechanical Engineering
7-1 Oogigaoka, Nonoichi, Ishikawa, 921-8501, Japan
y-sugi@neptune.kanazawa-it.ac.jp

Keywords: Cavitation, Cloud cavitation, Re-entrant motion, Propagation of bubble collapse, Image analysis

Abstract

It is known that cloud cavitation shows a periodic shedding behavior and causes high impacts. A re-entrant motion plays an important role in the shedding of cloud cavitation (for example, Knapp, et al 1970, Franc & Michel 2004). We have also performed some detailed observations on the shedding motion and the re-entrant motion of cloud cavitation (Sato & Saito 2006). A periodic behavior of cloud cavitation and the accompanying re-entrant motion can be observed with the propagation of bubble collapses in a two-phase flow condition. We also show a possibility that the collapse of cloud cavitation causes the re-entrant motion. In this study, we present some results from detailed observations and measurements on the collapse of cloud cavitation and the pressure waves using an image analysis technique. In addition, we show a starting mechanism of the periodic behavior of the re-entrant motion.

Introduction

It is known that cloud cavitation generated on a separated shear layer like a hydrofoil shows a periodic shedding behavior and causes high impacts. There are many experimental and numerical studies on such unsteady cloud cavitation (e.g., Knapp, et al 1970, Franc & Michel 2004, Kawanami, et al 1997, Arndt, et al 2005). The authors also study on behaviors of cloud cavitation in a separated shear layer on a convergent- divergent nozzle channel. We show that cavitation clouds show pairing and coalescence motion in the periodic growing process (e.g., Sato & Saito 2006, Sato, et al 2003, Saito & Sato 2003).

A re-entrant motion plays an important role in the shedding of cloud cavitation (e.g., Knapp, et al 1970, Franc & Michel 2004, Kawanami, et al 1997). The generation mechanism of a re-entrant motion which causes periodic shedding of cloud cavitation is a jet or flow from the trailing edge of attached cavity near reattachment region to the leading edge. On the other hand, the authors show that the re-entrant motion is not only a jet or flow but also propagation of bubble collapse (Sato, et al 2003). In addition, the authors also suggest that the trigger of re-entrant motion is pressure wave by the collapse of cloud cavitation (Sato & Saito 2006).

We try to estimate the mechanism of unsteady behavior of cloud cavitation with an image analysis. As for the image analysis techniques for cavitation study, Pham et al (1999) show an unsteady behavior of cloud cavitation on a hydrofoil. Kobayashi et al (2005) show vortex cavitation on the jet boundary by estimating cavitating region. Dular et al (2006) investigate the time average cavitating region in relation to the erosion distribution. These examples show changes in the area of cavitating region.

In this study, we focus on not only changes in cavitating region but also behaviors of surrounding small bubbles from many observations using a high speed video camera. Here, we analyze high speed phenomena using an image analysis related to the chain reaction of bubble collapses. We show the image analysis method together with its usefulness. Then applying these techniques to cavitating flow condition, we try to estimate the re-entrant motion and the propagation of bubble collapses quantitatively.

Nomenclature

Fs	Recording speed of high-speed video-camera (fps: frames per second)
H	Height of nozzle (mm)
P	Upstream pressure (Nm^{-2})
Pv	Vapor pressure (Nm^{-2})
Re	Reynolds number
Tw	Temperature of water (K)
U	Upstream velocity (ms^{-1})
x	Streamwise coordinate (mm)

Greek letters

β	Dissolved oxygen content ($mg\ell^{-1}$)
ν	Kinematic viscosity (m^2s^{-1})
θ	Divergent angle (deg)
ρ	Density of water (kgm^{-3})
σ	Cavitation number

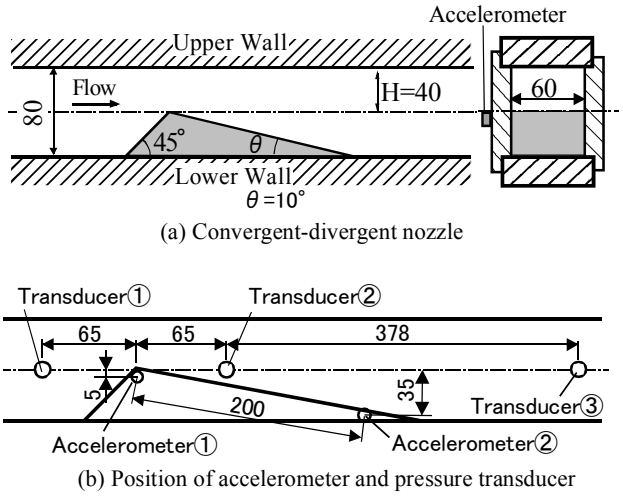

(a) Convergent-divergent nozzle

(b) Position of accelerometer and pressure transducer

Figure1: Test section.

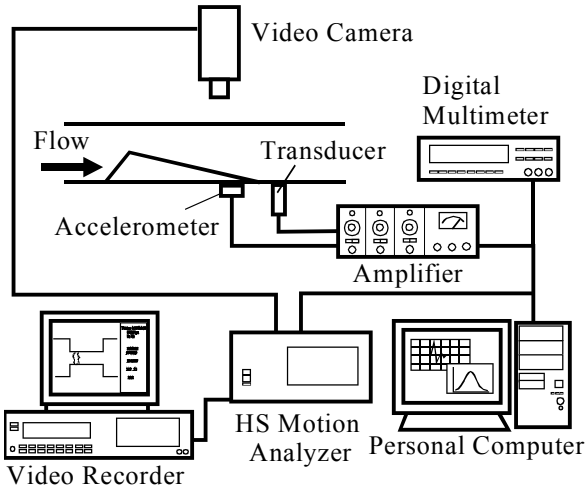

Figure 2: Measurement system.

Experimental Apparatus and Procedure

A closed-type cavitation tunnel is used for experiments. The test section has a rectangular cross section of 80 mm in height and 60 mm in width as shown in Fig. 1(a). A convergent-divergent nozzle with convergent angle of 45 degrees and divergent angle of 10 degrees is installed in the full width of the test section. An accelerometer (TEAC 703FB) is installed on the outside wall at the throat or the trailing edge of nozzle in the test section as shown in Fig.1(b). Pressure transducers (JTECT PMS-5) are also installed in the upstream and downstream of the nozzle in order to measure pressure fluctuation by bubble collapses. Collapse behavior of cloud cavitation is observed by a high-speed video-camera (Photron EKTAPRO4540) triggered by an impulsive acceleration pulse from the accelerometer (see Fig.2). Cavitation is generated by decreasing the tunnel pressure under constant flow velocity condition (U=3.6m/s).

Cavitation number σ and Raynolds number Re are defined as follows,

$$\sigma=2(P-P_v)/\rho U^2 \quad (1)$$

$$Re=U \cdot H/\nu \quad (2)$$

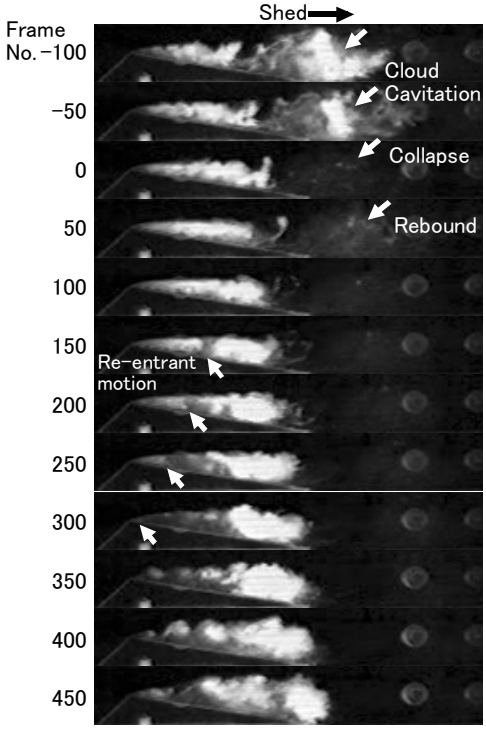

σ=7.5 U=3.6m/s β=2.7mg/ℓ Tw=293K Fs=9000fps

Figure 3: Behavior of shedding and re-entrant motion in cloud cavitaion.

where P and U are static pressure and flow velocity upstream of the nozzle, respectively. Pv, ρ and ν are vapor pressure, density and kinetic viscosity of water, respectively. β and Fs are air (oxygen) content and recording speed of the high-speed video-camera, respectively.

Image Analysis Method

Since collapses of bubble cloud cause a chain-reaction motion of small bubbles collapse, some gradation appears on an image (gray scale image). In this study, an image analysis technique is applied to these images in order to quantitatively estimate the behavior of cloud cavitation.

The 265 gradation images with 256x256 pixels can be taken by the high-speed video-camera. In the case of recording speed at 9000 frames per second, the size of image is 256x128 pixels. Figure 3 shows a series of images with 231x34 pixels corresponding to the area of test channel.

Here, in order to estimate the behaviors of cloud cavitation in a streamwise direction, we calculate an average gray level in the vertical direction of each image and show a gray level profile in the streamwise direction as shown in Fig. 4(a). Figure 4(b) shows a result of time-series analysis of those images. Contour map of the gray level profile is also shown in Fig.4(c). In the Fig. 4(c), a colored region from yellow to red indicates a cavitating zone. We can find the behavior of cavity shedding at the upper right part of Figs. 4(a), (b). We can observe the growth of attached cavitation in the upstream region (x<250). Then, we can also observe a bubble collapse region corresponding to a re-entrant motion in the region of Frame No.0~350 and

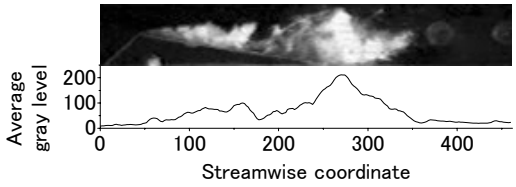

(a) Average gray level profile

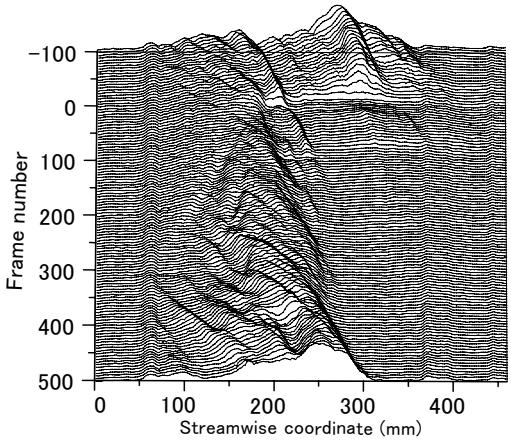

(b) Time series of average gray level profile

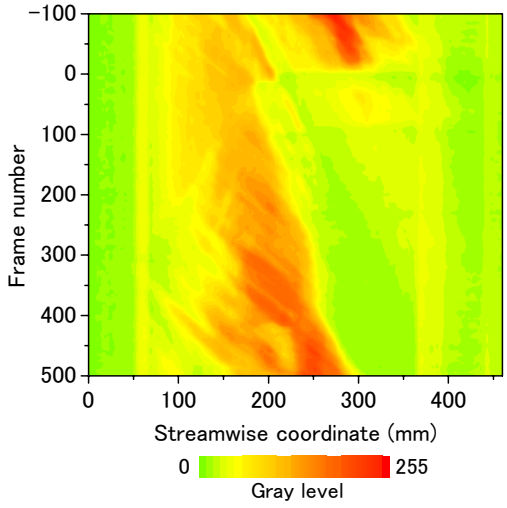

(c) Contour map of gray level profile

σ=7.5 U=3.6m/s β=2.7mg/ℓ Tw=293K Fs=9000fps

Figure 4: Results of simple image analysis.

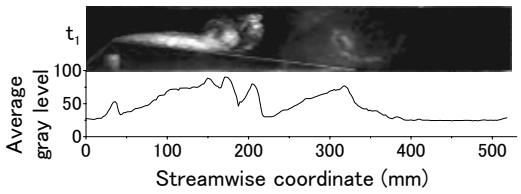

(a) Image and average gray level profile at t_1

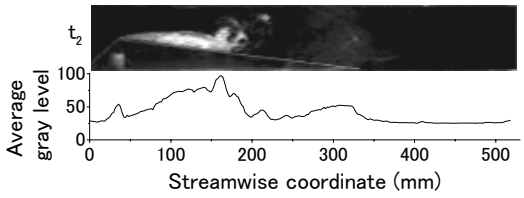

(b) Image and average gray level profile at t_2

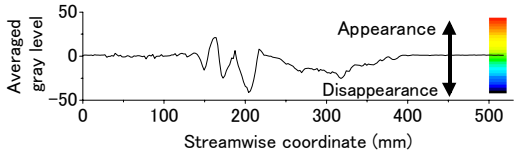

(c) Difference of gray level profiles (t_2-t_1)

Figure 5: Image analysis method with frame difference.

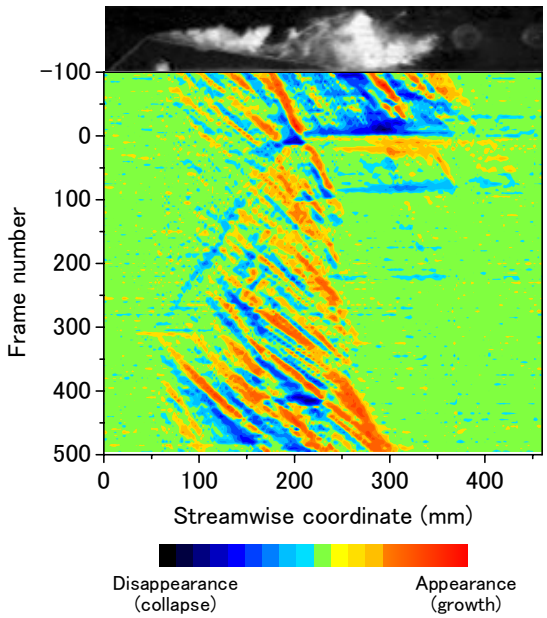

σ=7.5 U=3.6m/s β=2.7mg/ℓ Tw=293K Fs=9000fps

Figure 6: Diagram for shedding and re-entrant motion of cloud cavitation by frame difference method. (dt=5frames)

x=80~200.

Image Analysis Using Frame Difference

As mentioned above, we present that the behavior of cloud cavitation can be obtained using the image analysis. The difference between the gray levels of two images is calculated to clearly examine the change of bubble behavior. As shown in schematic diagram of Fig.5, the analysis is performed using two gray-scale images with 256 gradations. Originally the cavitating region is expressed as a white (indicated by value of 256) and the non-cavitating region as a black (indicated by value of 0). In this case, the bubble collapsing region which changes from the white to the black on the original pictures results in a positive value. Therefore, the positive value means the appearance/growth of cloud cavitation and the negative value means disappearance /collapse (in the case of cavity image with back light method, the analysis result is indicated by the opposite sign because the gradation of image is reversed). The advantage of this frame difference method is the clarification of change as well as that there is no necessity of background reduction and it is possible to analyze even when the lighting is not so uniform.

Figure 6 shows a result of the analysis by this method

at intervals of 5 frames. In the case of Fig.6, the bubble appearance region which changes from the black to the white on the original pictures is shown as red region as well as the collapse region is shown as blue region. The depth of color indicates the extent of change. It can be seen that the bubble collapse indicated by blue band propagates toward upstream. This behavior will be discussed in detail below.

Examination by Area of Analysis

Here, the analysis is preformed in the whole area of the channel. In the analysis, the cavitation behavior in the normal direction to the wall is neglected in order to estimate the cavity behavior in the streamwise direction. Naturally, the analysis region must be taken widely in the case of estimating the cavity behavior to all height of the channel. On the other hand, in the case of the analysis in local part, the local behavior can be examined clearly. It is necessary to adjust the analysis region to the phenomenon. So, we try to estimate the effect on the height of image.

The analysis is performed using the image over the whole channel height with 231x34 pixels. The images with 231x16, 231x8 and 231x2 pixels are also analyzed (see Fig.7). These images include the part of nozzle throat. Figure 8 shows a result of the analysis using these images by the frame difference method at intervals of 5 frames. Change of average gray level becomes lower with increase in the area of image. In the case of thin image, the result of average gray level profile shows extreme value. Since the analysis area is smaller, the result is affected by the gradation of local part. Therefore we can analyze a slight change in cavity behavior with thin image. In the case of cloud cavitation, we pay attention to the analysis because the cloud has complex surface and reflects the light irregularly.

Figure 9 shows a result of time-series analysis. The average gray level changes greatly with decrease in the analysis region. However, the re-entrant motion is clearly indicated by blue band (as shown in Fig.9 Frame No.0~300) running toward lower left direction. It is possible to estimate the behavior of cavity in local part by changing the region of the analysis.

Re-entrant Motion of Cavity and Propagation of Bubble Collapse

Behaviors of cloud cavitation generated on separated shear layer in the convergent-divergent channel flow are observed by a high-speed video camera triggered by an accelerometer installed on the outside wall of test section.

Figure 3 shows a typical example of shedding behavior of cloud cavitation. The shedding cloud cavitation (shedding cloud) collapses around Frame No.0 and shows rebound motion (Frame No.50). A re-entrant motion moves toward the leading edge of nozzle in the attached cavitation. The re-entrant motion reaches to the leading edge of the nozzle around Frame No.300, and then new attached cavitation begins to grow. Especially, there is a series of collapses of small bubbles remaining between attached cavitation and

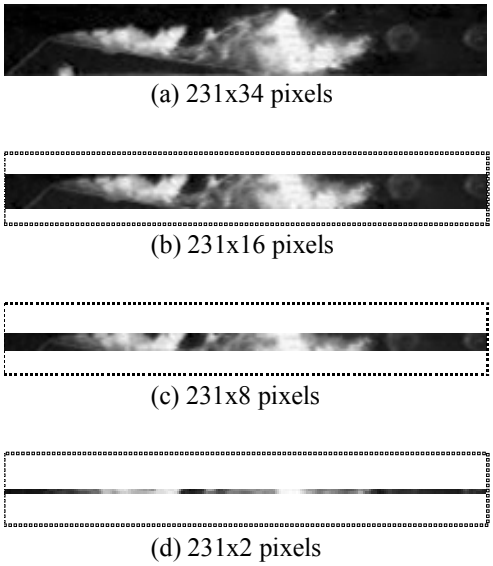

(a) 231x34 pixels

(b) 231x16 pixels

(c) 231x8 pixels

(d) 231x2 pixels

Figure 7: Various areas in analysis region.

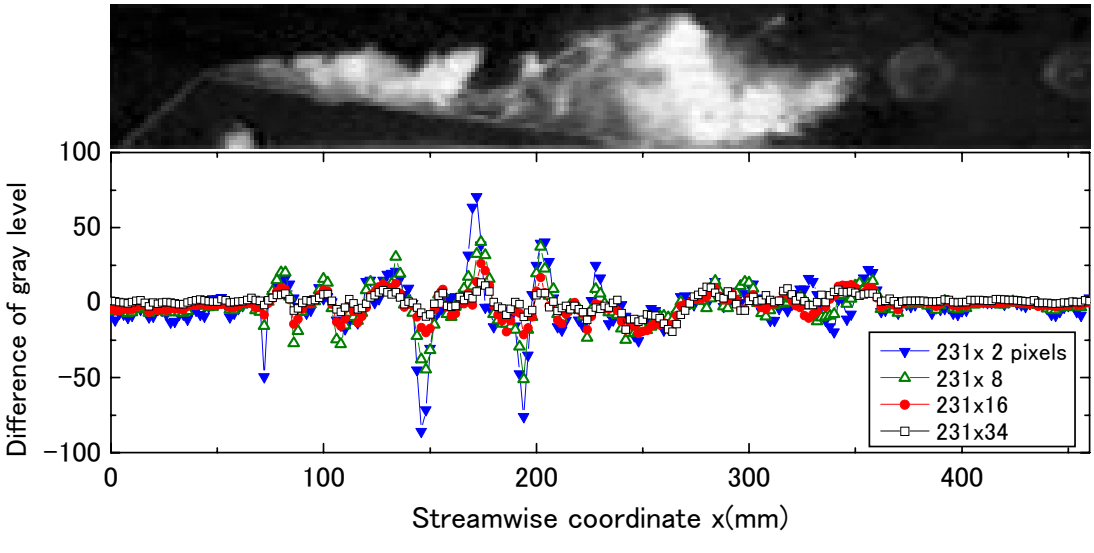

σ=7.5 U=3.6m/s β=2.7mg/ℓ Tw=293K Fs=9000fps

Figure 8: Result of image analysis with frame difference method in various analysis regions.

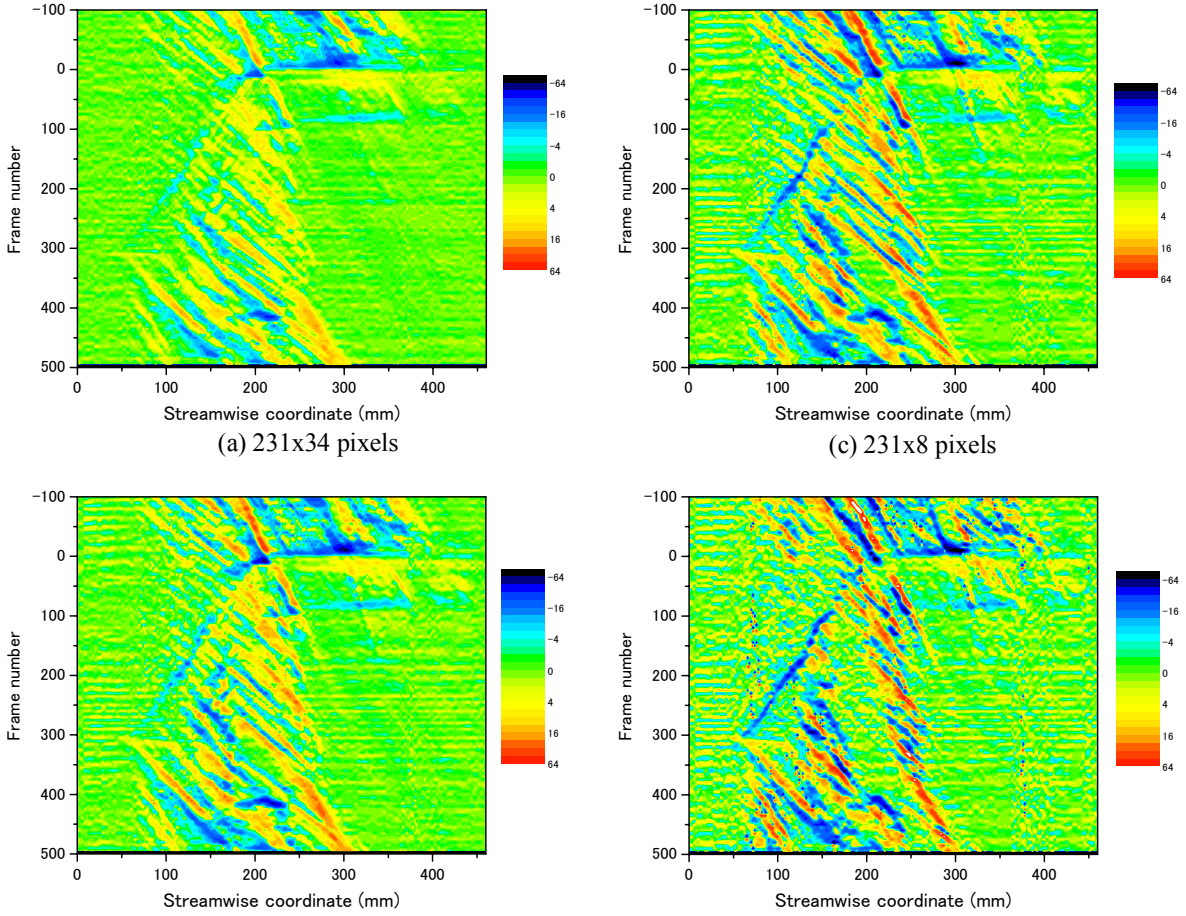

(a) 231x34 pixels

(c) 231x8 pixels

(b) 231x16 pixels

(d) 231x2 pixels

σ=7.5 U=3.6m/s β=2.7mg/ℓ Tw=293K Fs=9000fps

Figure 9: Effect of analysis region area.

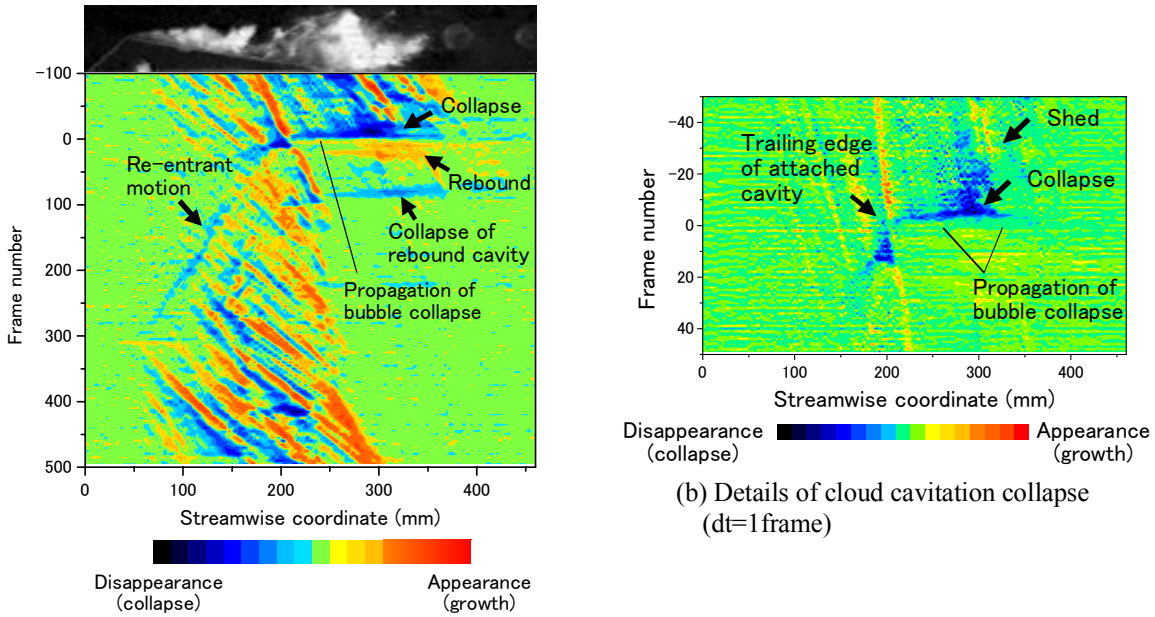

(a) Diagram of shedding and re-entrant motion of cavitaion clouds in frame difference method (dt=5frames)

(b) Details of cloud cavitation collapse (dt=1frame)

σ=7.5 U=3.6m/s β=2.7mg/ℓ Tw=293K Fs=9000fps

Figure 10: Shedding and re-entrant motion of cloud cavitation.

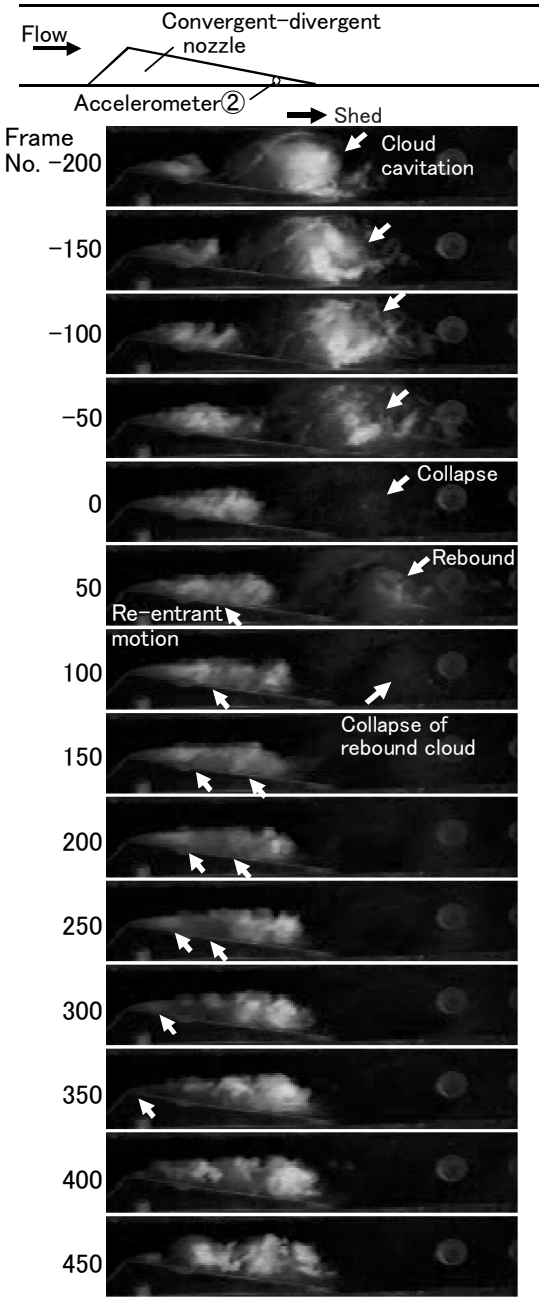

Figure 11: High speed video pictures of cloud cavitation and bubble collapse.

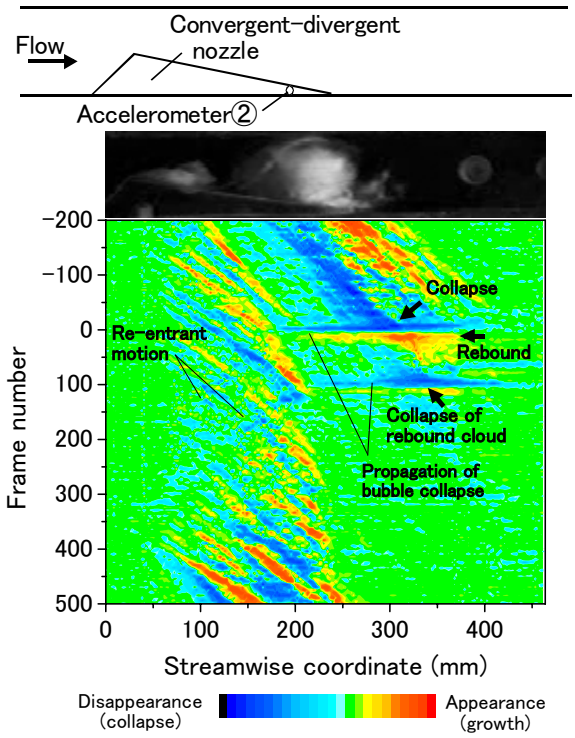

(a) Contour map in time series of gray level difference (dt=5frames)

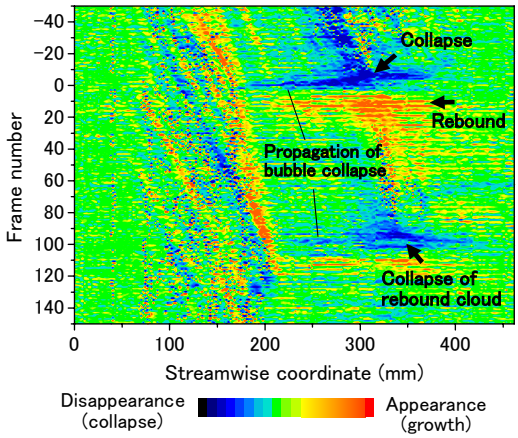

(b) Details of image analysis near cloud cavitaion collapse (dt=1frame)

σ=7.3 U=3.6m/s β=3.1mg/ℓ Re=1.4x10⁵ Tw=290K Fs=9000fps

Figure 12: Shedding and re-entrant motion of cloud cavitation.

shedding cloud. We try to display the bubble collapse behavior with the image analysis.

Figure 10(a) shows a result of the analysis using these images by the frame difference method at intervals of 5 frames. Therefore, in this case, the change in the period from 0.1 ms to 0.5 ms can be clearly displayed. Some lines toward lower right direction indicate the shedding cloud from Frame No.-100 to No.-20. Then the blue band indicates the collapse of shedding cloud around Frame No.0. And the blue region indicates the re-entrant motion toward lower left direction from Frame No.0 to No.300. As a result of these analyses, we can display a series of shedding behavior of cloud cavitation.

Figure 10(b) shows a result of the analysis using images from Frame No.-50 to No.50 in Fig.10(a) at interval of one frame in order to examine the collapse behavior of shedding clouds in detail. The blue region corresponding to collapse of shedding clouds can be observed in Frame No.-5 around streamwise coordinate x=300. It is also found that the blue band propagates toward upstream and downstream directions. This phenomenon corresponds to a series of collapse and propagation of surrounding small babbles by pressure wave generated by collapse of shedding cloud. In this case, the propagation speed toward upstream is estimated to be on the order of 200-300 m/s. As mentioned above, higher speed propagation behavior of bubble collapse can be estimated by analysis at shorter interval.

In addition, from the results in Figs.3 and 10, it is

found that the blue band corresponding to the propagation of bubble collapse reaches to the trailing edge of an attached cavity. Then the re-entrant motion begins to move toward upstream direction in the attached cavity.

Figures 11 and 12(a) show another typical example of propagation behavior of bubble collapse as well as a result of the analysis at intervals of 5 frames. Shedding clouds move toward downstream around Frame No.-200 to No.-50 and then it collapses around Frame No.0. At the time, the blue band corresponding to a series of collapse and propagation of surrounding small babbles reaches to the trailing edge of an attached cavity. After that the re-entrant motion begins to move. Furthermore the shedding clouds rebound as shown in Frame No.100 and collapse again. And then the other re-entrant motion as well as the propagation of bubble collapse can be observed.

Figure 12(b) shows a result of the analysis using the images by the frame difference method at intervals of one frame. The main cavity collapses around Frame No.0. Then a series of bubble collapses propagate upstream direction. In this case, the propagation speed toward upstream is estimated to be on the order of 200-300 m/s.

This result suggests that the re-entrant motion is triggered by the collapse of shedding clouds and the propagation of bubble collapse.

Re-entrant Motion and Propagation of Bubble Collapse

Figure 13 shows the final stage of the re-entrant motion which moves from the trailing edge toward the leading edge of the nozzle. The re-entrant motion of the cavity reaches to the leading edge of cavity around Frame No.0 in Fig.13(a). Around this time, pressure wave occurs and causes a chain-reaction of surrounding small bubbles. Figure 13(b) shows an image analysis result on the propagation of bubble collapse when the re-entrant motion reaches to the leading edge. The blue band expands to lower right direction around Frame No-2 to No.2. This indicates the propagation of bubble collapse accompanying the propagation of pressure wave. The propagation speed is estimated to be about 150 m/s.

Figure 13(c) shows fluctuations of pressure as well as impulsive acceleration. The impulsive pulse from an accelerometer occurs at Frame No.0. This means that the collapse of cavities near the nozzle throat, that is, the re-entrant motion reaches to the leading edge of the nozzle. The pressure from the pressure transducer 1 installed upstream of nozzle begins to rise around Frame No.-2. It is found that the pressure wave propagates towards upstream by the fact that the bubbles in an attached cavity begin to collapse as shown in the result of image analysis of Fig.13(b). Since the pressure rise appears around Frame No.1 in the pressure transducer 2 installed in x=80, it is found that pressure wave propagate towards downstream. These results correspond to the results of the image analysis as mentioned previously.

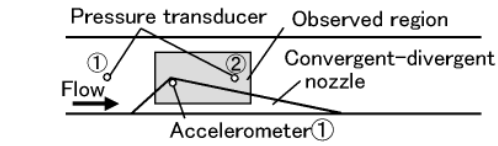

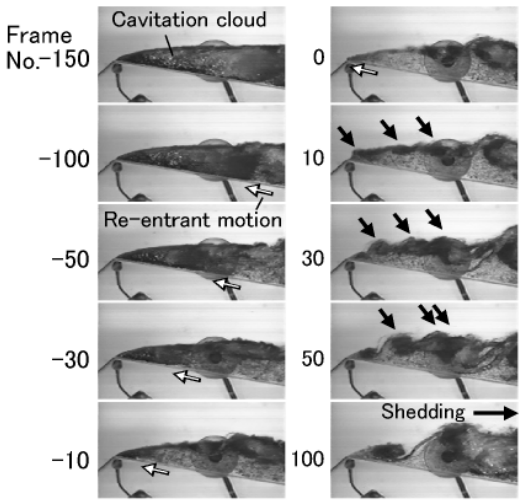

(a) Behavior of re-entrant motion

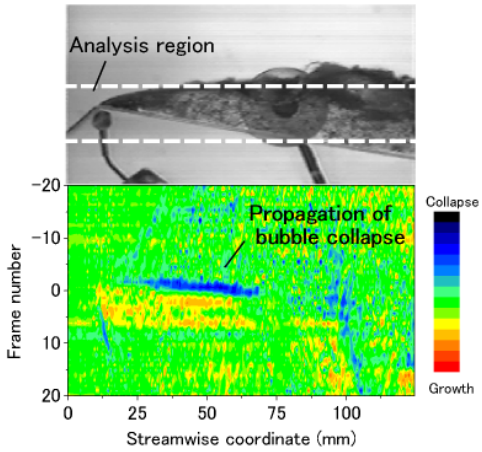

(b) Propagation behavior of bubble collapse by frame difference method

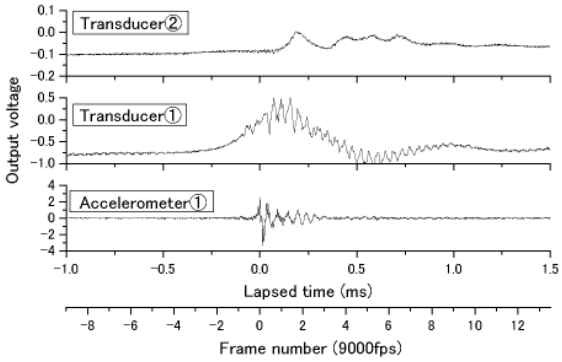

(c) Impulsive acceleration and pressure fluctuation

σ=7.5 U=3.6m/s β=2.7mg/ℓ Tw=293K Fs=9000fps

Figure 13: Behavior of re-entrant motion and propagation of bubble collapse.

Conclusions

1) High-speed phenomenon related to unsteady cloud cavitation can be described using an image analysis. Especially, the frame difference analysis method in the present study can quantitatively estimate a series of

unsteady behaviors such as cloud shedding, collapsing and re-entrant motion as well as propagation of bubble collapses.
2) Using the image analysis and the pressure measurement we show that pressure wave can occur at the collapse of shedding clouds and a chain reaction of surrounding small bubble collapses can occur.
3) It is indicated that the re-entrant motion can be triggered by collapse of shedding clouds and propagation of bubble collapse.

Acknowledgements

The authors are grateful to Mr. Yoshihisa Abe and Mr. Keito Yamakita who were students in Department of Mechanical Engineering in Kanazawa Institute of Technology for carrying out the experiments and analyses.

References

Arndt, R. E. A., et al., Control of Cavitating Flows: A Perspective, JSME International Journal Series B, Vol. 48, No. 2, pp.334-341, (2005).

Dular, M. et al., Development of a cavitation erosion model, Wear, 261, 642-655, (2006).

Franc, J.P. and Michel, J.M., Fundamentals of Cavitation, Kluwer Academic Publishers, (2004).

Kawanami, Y. et al., Mechanism and Control of Cloud Cavitation, Vol.119, J. Fluid Eng., Trans. ASME, pp.788-794, (1997).

Knapp, R.T. et al., Cavitation, McGraw-Hill, (1970).

Kobayashi, et al., Unsteady behavior of Cavity Boundary Directly Related to Cavity Discharge, J. JSME, Ser. B, Vol. 71, No.703, pp.804-810, (2005). (in Japanese)

Pham, T. M. et al., Investigation of Unsteady Sheet Cavitation and Cloud Cavitation Mechanism, J. Fluid Eng., Trans. ASME, Vol.121, (1999), pp.298-296.

Saito, Y. and Sato, K., Growth Process To Cloud-Like Cavitation On Separated Shear Layer, Cavitation and Multi-Phase Flow Forum, ASME, FEDSM2003-45007, (2003).

Sato, K. and Shimojo, S., Detailed Observations on a Starting Mechanism for Shedding of Cavitation Cloud, Fifth International Symposium on Cavitation (CAV2003), Cav03-GS-4-009, (2003).

Sato, K., Shimojo, S. and Watanabe, J., Observations of Chain-reaction Behavior at Bubble Collapse using Ultra High Speed Video Camera, Cavitation and Multi-Phase Flow Forum, ASME, FEDSM2003-45002, (2003).

Sato, K., and Saito, Y., High-speed Video observation on Mechanism of Re-entrant motion and Cloud Shedding in Cloud Cavitation, The 5th International Symposium on Measurement Techniques for Multiphase Flow, Macau,Vol. II, pp. 1089-1093, (2006).